

Nanomanipulation of single influenza virus using dielectrophoretic concentration and optical tweezers for single virus infection to a specific cell on a microfluidic chip

Hisataka Maruyama · Kyosuke Kotani ·
Taisuke Masuda · Ayae Honda · Tatsuro Takahata ·
Fumihito Arai

Received: 15 August 2010 / Accepted: 14 November 2010 / Published online: 1 December 2010
© Springer-Verlag 2010

Abstract A major problem when analyzing bionanoparticles such as influenza viruses (approximately 100 nm in size) is the low sample concentrations. We developed a method for manipulating a single virus that employs optical tweezers in conjunction with dielectrophoretic (DEP) concentration of viruses on a microfluidic chip. A polydimethylsiloxane microfluidic chip can be used to stably manipulate a virus. The chip has separate sample and analysis chambers to enable quantitative analysis of the virus functions before and after it has infected a target cell. The DEP force in the sample chamber concentrates the virus and prevents it from adhering to the glass substrate. The concentrated virus is transported to the sample selection section where it is trapped by optical tweezers. The trapped virus is transported to the analysis chamber and it is brought into contact with the target cell to infect it. This

paper describes the DEP virus concentration for single virus infection of a specific cell. We concentrated the influenza virus using the DEP force, transported a single virus, and made it contact a specific H292 cell.

Keywords Nanomanipulation · Influenza virus · Dielectrophoretic force · Optical tweezers · Microfluidic chip

1 Introduction

Nanobiomanipulation for virus and DNA analysis has become one of the most important topics in nanobiotechnology in recent years (Amato 2005). The ability to manipulate a single virus is necessary to analyze the functions of influenza virus such as cell infection and incubation in a cell. Cultured cells have conventionally been used to analyze viral functions (Parvin et al. 1989). Although this method can acquire average information from many cells, the properties of individual infected cells vary depending on their physiological states and cell cycle. The efficiency of viral infection also varies between cells. Moreover, viral proliferation depends on the function of the nucleus of the infected cell. To perform quantitative analysis of a virus, single virus infection of a specific cell is required. However, there are some problems such as manipulation and preparation of nanobiomaterials for experiment. Low sample concentration is one of the most important problems because biomaterials such as viruses are scarce.

Methods for manipulating biomaterials on an optical microscope, an atomic force microscope, and a scanning electron microscope have been developed (Castillo et al. 2009). It is desirable to manipulate biomaterials in a wet

H. Maruyama (✉) · T. Masuda
Department of Mechanical Science and Engineering, Nagoya University, Furo-cho, Chikusa-ku, Nagoya 464-8603, Japan
e-mail: hisataka@mech.nagoya-u.ac.jp
URL: <http://www.biorobotics.mech.nagoya-u.ac.jp>

F. Arai
Department of Micro-Nano Systems Engineering, Nagoya University, Furo-cho, Chikusa-ku, Nagoya 464-8603, Japan

K. Kotani
Department of Bioengineering and Robotics, Tohoku University, Aramaki Aoba 6-6-01, Aoba-ku, Sendai 980-8579, Japan

A. Honda · T. Takahata
Department of Frontier Bioscience, Hosei University, Kajino-cho 3-7-2, Koganei 184-8584, Japan

F. Arai
Core Research for Evolutional Science and Technology, Japan Science and Technology Agency, Saitama, Japan

condition to maintain their activity. Moreover, manipulation in a closed space such as a microfluidic chip is also desirable to prevent environmental disturbances. In recent years, microfluidic chips have been used to manipulate biomaterials (Arai et al. 2001). Some form of non-contact manipulation is required for on-chip manipulation because it is quite difficult to insert mechanical manipulators in chips.

Various forms of non-contact manipulation including fluidic force, magnetic force, electrical force, and optical tweezers have been developed for on-chip manipulation in microfluidic chips. Hydrodynamic force has several advantages including low cost, low power consumption, and the potential for parallel operation (Kim et al. 2008). However, it is difficult to use hydrodynamic force to perform selective manipulation of a single target. Magnetic force is considered to be safe for biomaterials (Kuhara et al. 2004). However, to manipulate a single target it is necessary to modify it by incorporating a magnetic material because most biomaterials are nonmagnetic. Although it is possible to concentrate biomaterials, concentrated samples can be modified by magnetic materials. Electrophoresis and dielectrophoresis are important means for performing biomanipulation (Schnelle et al. 2000). They are suitable for manipulating many samples, but it is difficult to use them to manipulate a single sample. Optical tweezers have been used in biology and they have been employed to manipulate biomaterials such as cell, virus, and DNA (Arthur et al. 1986). They are capable of manipulating single targets, but they have low throughputs. Thus, to concentrate and perform stable manipulation of biomaterials, a combination of some of the above methods is required.

We have proposed “on-chip robotics” for integrating micro and nanomanipulation and performing measurements on a microfluidic chip (Arai et al. 2003; Ichikawa et al. 2005; Maruyama et al. 2005, 2008). A Robochip is a microfluidic chip in which micro/nano robots are installed and which can perform single-cell measurements and analysis, dispense droplets, cloning, and anatomical manipulation for on-chip micromanipulation such as cell sorting (Yamanishi et al. 2008; Shinya et al. 2009). Robochips have many advantages such as being rapid, highly accurate, and disposable, enabling local environmental control, and being robust against disturbances (Ichikawa et al. 2007).

In a previous study, we manipulated a single virus and used it to infect a specific cell in a microfluidic chip (Ichikawa et al. 2007). The chip has a virus chamber and a cell culture chamber. An influenza virus was transported from the virus chamber to the cell culture chamber by optical tweezers on a gel microbead made of poly(*N*-isopropylacrylamide) (Ishikawa et al. 1993). Although single virus infection could be performed, it was quite difficult and time consuming. The chip has no flow control since the

cell culture chamber is not isolated from the virus chamber, making it possible for other viruses beside the intended virus to infect the target cell. We subsequently developed a chip with high-speed flow control (Arai et al. 2009) and in which the virus chamber was isolated from the cell chamber. However, it was still difficult to use this chip because of the low virus concentration in the chip.

In the present study, we infected a specific cell with a single virus by manipulating the virus using optical tweezers in conjunction with dielectrophoretic (DEP) concentration of the virus in a microfluidic chip. The microfluidic chip has a sample chamber and an analysis chamber. Viruses were injected into the sample chamber and were concentrated by DEP force. For DEP concentration, the conductivity of the solution was adjusted to 10 mS/m to prevent thermal damage. The virus selected from the concentrated group was trapped and transported to the analysis chamber by optical tweezers. The virus was brought into contact with the selected cell to infect it. We demonstrate DEP concentration of influenza viruses and contact with a specific cell in the chip.

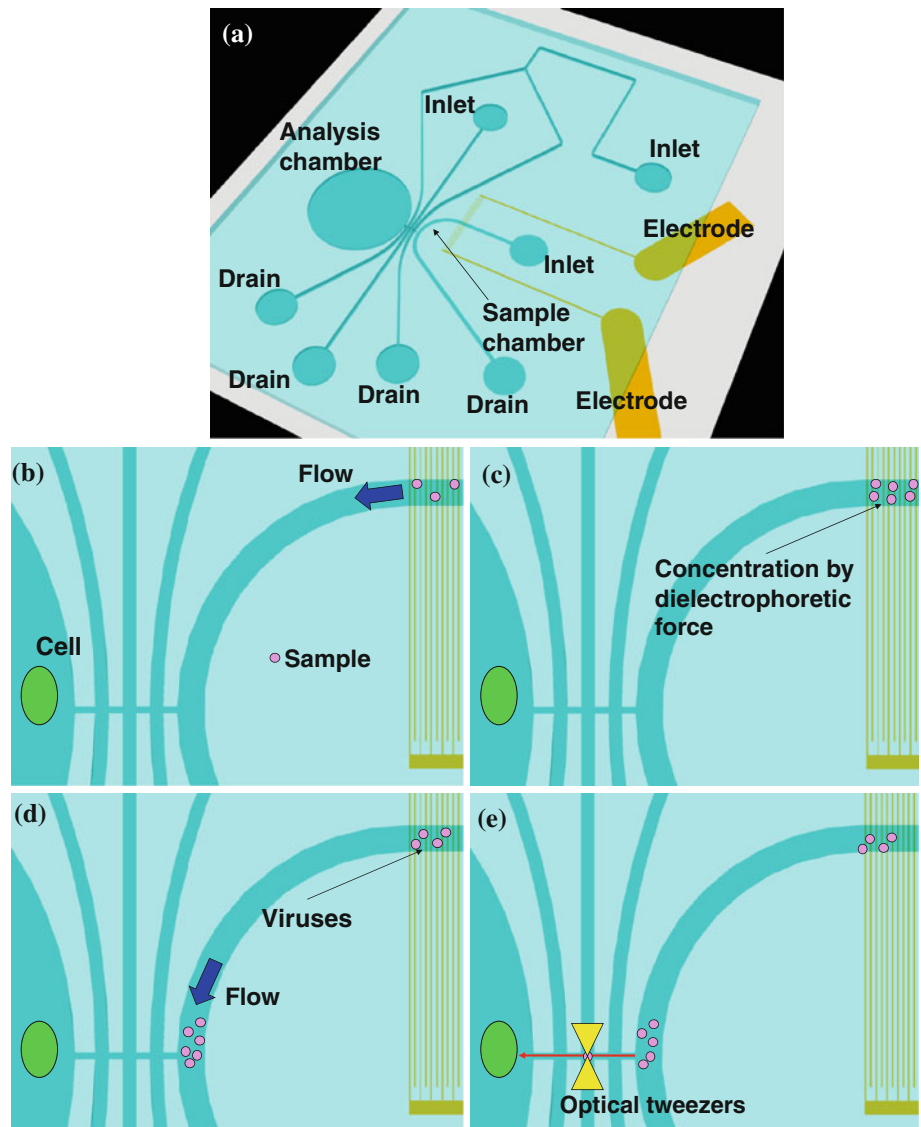
2 Materials and methods

2.1 Microfluidic chip for infecting a specific cell with a single virus using DEP concentration

Figure 1 shows a schematic of on-chip infection of a specific cell with a single virus. The microfluidic chip consists of a sample chamber, electrodes for concentrating viruses, an analysis chamber, and microchannels for buffer flow (Fig. 1a). Viruses were stained with a fluorescent dye to enable them to be observed. The surfaces of the microchannels and chambers were pretreated with bovine serum albumin (BSA) to prevent viruses adhering to the chip. Each inlet port was connected to the syringe pump through the solution reservoir. The top of the analysis chamber was sealed by a self-adhesive material such as polydimethylsiloxane (PDMS). After single virus infection had been performed, the cell could be extracted by opening the analysis chamber.

Figure 1b–e depicts the process of single virus infection using DEP concentration and optical tweezers. The virus solution was first loaded into the sample chamber and the buffer was simultaneously injected as sheath flow. The viruses were concentrated on the electrodes by DEP force. Viruses were concentrated by generating a negative DEP force through adjusting the conductivity of the solution and the frequency of the voltage. The DEP force also prevents the viruses from adhering to the chip. A single virus was selected from the concentrated group and it was trapped and transported to the analysis chamber using optical

Fig. 1 Schematic of single-cell infection of a specific cell using DEP concentration and optical tweezers in a chip. **a** Schematic of microfluidic chip. **b** Virus injection into sample chamber. **c** Virus concentration by DEP force. **d** Flow of concentrated viruses to selection region. **e** Transport of single virus to analysis region and contact with a specific cell for infection



tweezers. This virus loading method reduces the consumption of the scarce sample because it is difficult to detect viruses at low concentrations. The transported virus was brought into contact with the target cell to infect it. After infection by the required number of viruses, these chambers can be isolated by stacking using a photo-crosslinkable resin to prevent other viruses from entering the analysis chamber (Müller et al. 1996). Viruses outside the analysis chamber cannot enter the chamber due to physical blocking by the polymerized resin.

2.2 DEP concentration of viruses in microfluidic chip

We used DEP force for virus concentration because the virus was present in a low concentration. Figure 2 shows a schematic diagram of the electrodes. The electrodes are 10 μm wide and the gap between them is 30 μm. The concentration of the virus in the solution was 1×10^6

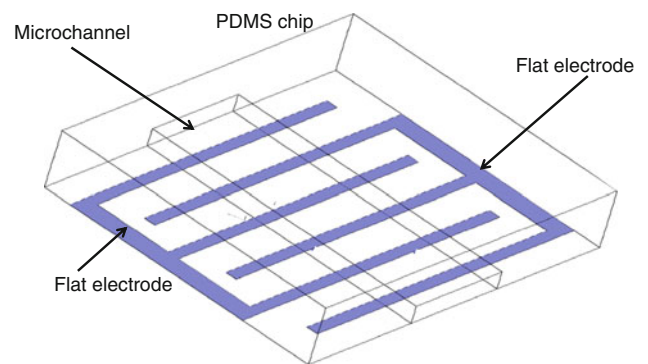


Fig. 2 Analytical model

viruses/μl; this low-virus concentration made it difficult to observe the virus in the sample chamber since on average, there were less than 0.1 viruses in the field of view. A high-frequency voltage was applied to the electrodes to generate

the DEP force. The effect of the DEP force on the viruses depends on the electric field gradient between the electrodes. The DEP force is given by the following equations:

$$F_{\text{DEP}} = 2\pi\epsilon_m r^3 \text{Re} \left[\frac{\epsilon'_p - \epsilon'_m}{\epsilon'_p + 2\epsilon'_m} \right] \nabla |E|^2 \quad (1)$$

$$\epsilon'_p = \epsilon_p - j \frac{\sigma_p}{\omega} \quad (2)$$

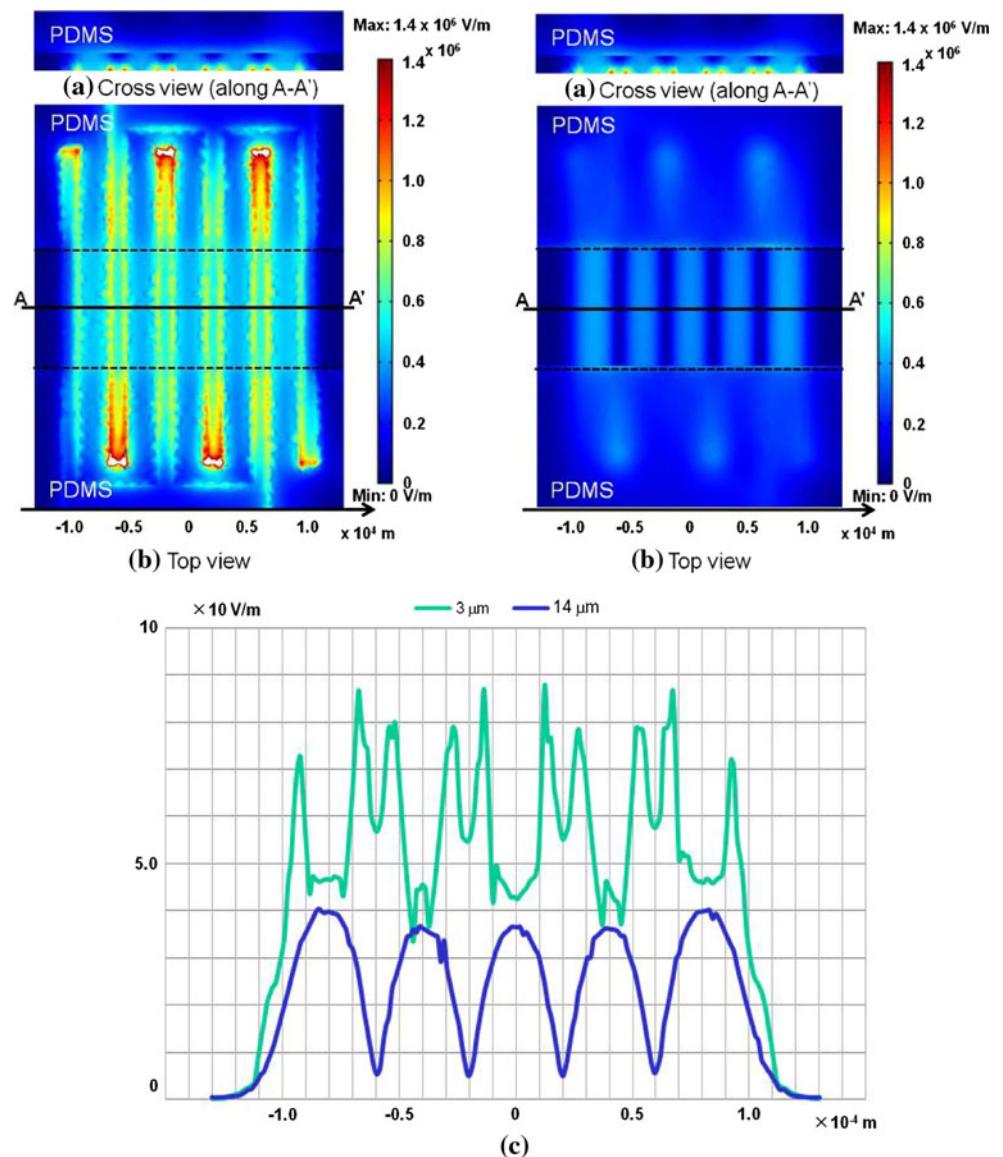
$$\epsilon'_m = \epsilon_m - j \frac{\sigma_m}{\omega} \quad (3)$$

where E is the electric field strength, r is the particle radius, ϵ'_p and ϵ'_m are, respectively, the complex permittivities of the particle and the solution, ϵ_p and ϵ_m are, respectively, the permittivities of the particle and the solution, σ_p and σ_m are, respectively, the conductivities of the particle and the solution, and ω is the angular frequency of the voltage. If ϵ'_p

is smaller (larger) than ϵ'_m , the negative (positive) DEP force causes the particles to move in the direction of decreasing (increasing) gradient. ϵ'_p and ϵ'_m depend on the frequency ω .

We analyzed the electric field distribution by the finite element method (FEM) using commercial software (Comsol Multiphysics, Comsol AB). In this analysis, the electric field distribution in water was analyzed. Figure 2 shows the model used for the FEM analysis. The microchannel was 200 μm wide and 15 μm high. The electrodes were 10 μm wide and 600 μm long and there was a 30 μm gap between them. The permittivities of PDMS and water were 2.67 and 81.0, respectively. Figure 3a shows the FEM results for the electric field distribution and Fig. 3b shows the electric field distributions along the center of the microchannel (i.e., line AA') at two different heights. For both heights, the electric field gradient was high at the edge of

Fig. 3 FEM results for the electric field distribution. Electric field distributions at **a** 3 μm and **b** 14 μm from electrodes. **c** Comparison of electric field distributions at two different heights



the electrode. In contrast, it was low between the electrodes and at the center of the electrodes. A positive DEP force may cause thermal damage to the sample due to the heat generated by the electrode. To prevent this, we adjusted the frequency to generate a negative DEP force so as to concentrate the viruses between the electrodes.

A high frequency (3 MHz) was employed for DEP manipulation of a virus according to the previous study (Müller et al. 1996). We assumed that the virus was spherical with a diameter of 100 nm (Stanley 1944). The permittivity of the virus was taken to be 2 and its conductivity was taken to be the same as that of the solution. The solution conductivity was adjusted to 10 mS/m to prevent thermal damage to the sample and electrodes. Under these conditions, the virus experienced a negative DEP force because $\text{Re}\{(\epsilon'_p - \epsilon'_m)/(\epsilon'_p + 2\epsilon'_m)\}$ was negative (−0.47).

A negative DEP force also prevents the viruses adhering to the glass surfaces since it operates upward from the glass substrate. The virus moves by Brownian motion. The virus will not adhere to the glass surface if the DEP force exceeds the Brownian force. The Brownian force is given by:

$$F_B = m_v \times \langle \dot{x} \rangle = \frac{4}{3} \rho_v \pi a^3 \times \sqrt{\frac{RT}{3\pi\eta a N_A}} \tag{4}$$

where F_B is the Brownian force, ρ_v is the virus density, a is the virus radius, R is the molar gas constant (8.31447 J K^{−1} mol^{−1}), T is the temperature, η is the viscosity of the solution (1.004 × 10^{−6} m²/s), and N_A is the Avogadro constant. We compared the two forces at a height of 50 nm above the glass substrate. We assumed that the virus density was 1 g/cm³. From Eq. 2, the minimum F_{DEP}

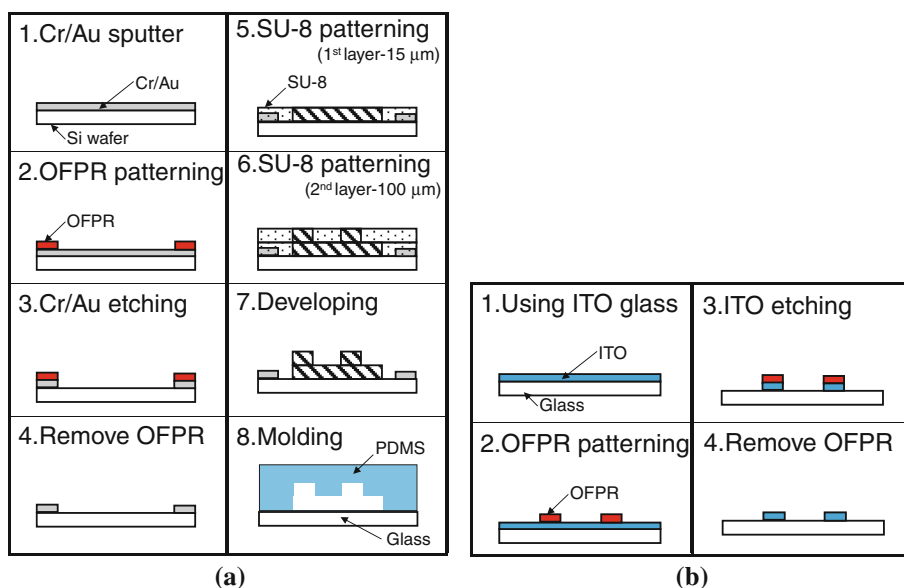
is 6.69 × 10^{−6} N. From Eq. 3, F_B was 1.53 × 10^{−24} N. Therefore, we concluded that the virus will not adhere to the glass surface since the negative DEP force exceeds the Brownian force.

2.3 Fabrication of microfluidic chip

Figure 4 depicts the process used to fabricate the microfluidic chip. A PDMS chip was fabricated by photolithography and replica molding. Chip molds were fabricated by multiexposures to fabricate chips that have areas with different heights. A Cr/Au layer was sputtered on a Si wafer. A positive photoresist (OFPR, Tokyo Ohka Kogyo Co. Ltd) was spin coated and patterned to fabricate an alignment pattern for multiexposure of a negative resist (SU-8, Kayaku Microchem). After removing the developed OFPR, the Cr/Au layer was etched. The SU-8 sheet was then coated and patterned. This mold has two areas with different heights: one area was 15 μm thick and it was for the sample chamber, while the other area was 115 μm thick and it was for microchannels and the analysis chamber. The sample chamber was 200 μm wide. The microchannels were 100 μm wide. The analysis chamber was 5 mm in diameter. The top of the analysis chamber was sealed with a PDMS membrane to allow the sample chamber to be opened for inserting and removing cells.

Figure 4b shows the fabrication process for the electrodes. A Cr/Au layer was sputtered on the Si wafer. A positive photoresist OFPR was then spin coated and patterned to fabricate the pattern for the electrodes. The photoresist was removed after the Cr/Au layer had been etched by FeCl₃ solution.

Fig. 4 Fabrication process of microfluidic chip. Fabrication processes of **a** microchannel and **b** glass substrate with electrodes



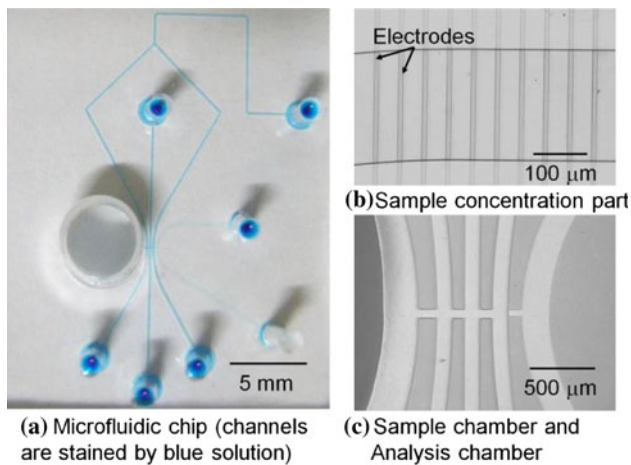


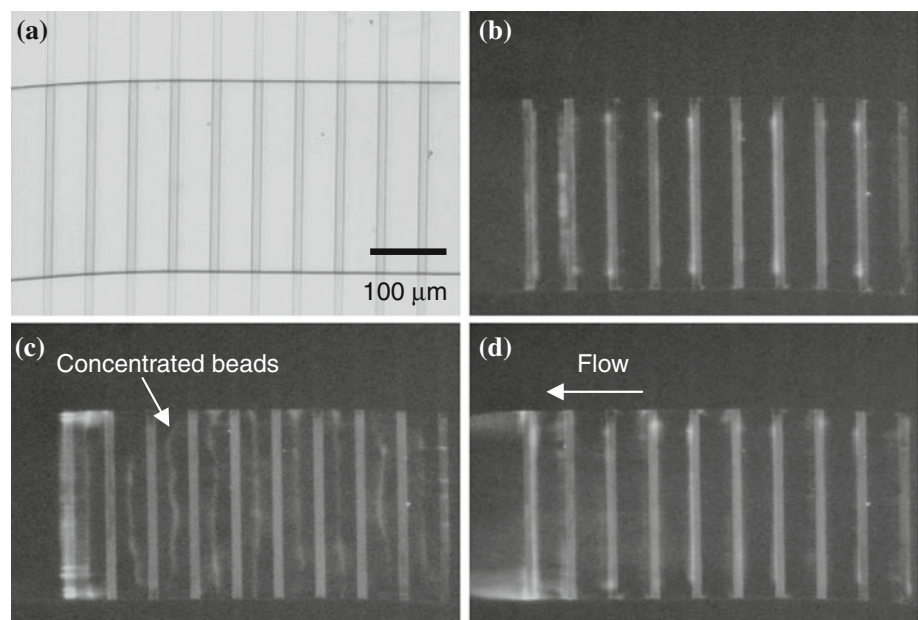
Fig. 5 Photographs of microfluidic chip. **a** Microfluidic chip (channels are stained by blue solution). **b** Sample collection region. **c** Sample chamber and analysis chamber

Figure 5 shows photographs of the sample chamber; it has a sample concentration region and a sample selection region. We could culture H292 cells in the analysis chamber.

2.4 Experimental setup

We used an inverted microscope (IX71, Olympus) equipped with an epifluorescence system. Fluorescent polystyrene (PS) beads (excitation wavelength: 491 nm; emission wavelength: 515 nm) were injected into the sample chamber using a syringe pump (KDS120, KDScientific Co. Ltd.) to confirm DEP concentration. The flow rate was 0.10 $\mu\text{l/h}$. A high-frequency voltage was applied to the electrodes by a function generator (WF1974, NF Corporation). The fluorescence intensity of the PS beads was

Fig. 6 Results of DEP sample concentration in microfluidic chip. **a** Sample injection to concentration part. **b** Fluorescence observation. **c** Particle concentration after 0.3 s. **d** Flow of concentrated particles



monitored using a color CCD camera (WAT-221, Watec Co. Ltd.) and recorded using a computer. We used a laser confocal microscope (A1R, Nikon Corporation) equipped with a laser manipulation system (maximum power: 1 W; output wavelength: 1064 nm) to perform DEP virus concentration and single virus infection of a specific cell.

Influenza viruses stained with a fluorescent dye (DiI; excitation wavelength: 549 nm; emission wavelength 565 nm) were used. DiI stains the virus membrane. 1 ml of DiI was mixed with 500 ml PBS(-). PBS(-) consists of 137 mmol/l NaCl, 2.68 mmol/l KCl, 8.1 mmol/l Na_2HPO_4 , and 1.47 mmol/l KH_2PO_4 . It has a pH of 7.4. The mixture is mixed with the virus suspension (DiI solution: virus suspension = 1:1). The viruses were incubated in the dark for 30 min. Finally, the virus solution was diluted by adding distilled water to adjust its conductivity to 10 mS/m. The virus concentration was 1×10^6 viruses/ μl .

We used a photo-crosslinkable resin, polyethylene glycol methacrylate (PEGMA), to isolate the sample chamber from the analysis chamber after viral infection had occurred. PEGMA is polymerized by ultraviolet light; ultraviolet light was generated by a mercury lamp in the microscope and controlled using a mechanical shutter.

3 Experimental results

3.1 Nanoparticle concentration by dielectrophoresis

We performed DEP concentration of fluorescent PS beads to confirm DEP virus concentration. The PS beads were 100 nm in diameter and had a permittivity of 2. Figure 6 shows the results of DEP concentration of fluorescent PS

beads. The initial PS bead concentration was 1.9×10^4 particles/ml. A square-wave voltage was applied with an amplitude of $20 V_{p-p}$. Frequencies in the range from 500 to 2000 Hz were used. We observed PS bead concentration between the electrodes by the negative DEP force. At a frequency of 2000 Hz, the fluorescence intensity was 1.26 times higher than that prior to concentration. After PS bead concentration had been performed for 10 s, the concentrated PS beads were transported to the sample selection region.

Figure 7a shows the results of calibrating the bead concentration with the fluorescence intensity. Based on this calibration, the PS bead concentration was increased from 1.9×10^4 particles/ml to 1.9×10^5 particles/ml by the negative DEP force. Figure 7b shows the relationship between the applied frequency (500, 800, and 2000 Hz) and the PS bead concentration. It shows that a frequency of 2000 Hz is suitable for concentrating PS beads.

3.2 Manipulation of single influenza virus on a chip

Figure 8 shows the experimental results for DEP concentration of influenza viruses using the microfluidic chip. The viruses were injected into the chip by a syringe pump. The flow rate was $0.10 \mu\text{l/h}$. A square wave was applied to the electrodes with amplitude of $20 V_{p-p}$ and a frequency of 3 MHz. Figure 8b shows that the viruses were concentrated

from 1×10^6 to 1×10^9 viruses/ μl . After 5 min of DEP concentration, we released the viruses by turning of the voltage. We then confirmed that no viruses had adhered to the glass substrate in the concentration area. Virus adhered to the glass surface when no DEP force was generated. This result demonstrates that DEP force is effective for concentrating viruses. After releasing the viruses, we transported them to the sample selection region.

Figure 9 shows the experimental results for the manipulation of a single virus by direct laser manipulation in the sample chamber using a laser micromanipulator (Sigma Koki). The laser power was set to 0.5 W to avoid photobleaching. Flow was stopped inside the chip. We succeeded in manipulating a single virus using optical tweezers. The maximum transport speed was approximately $10 \mu\text{m/s}$.

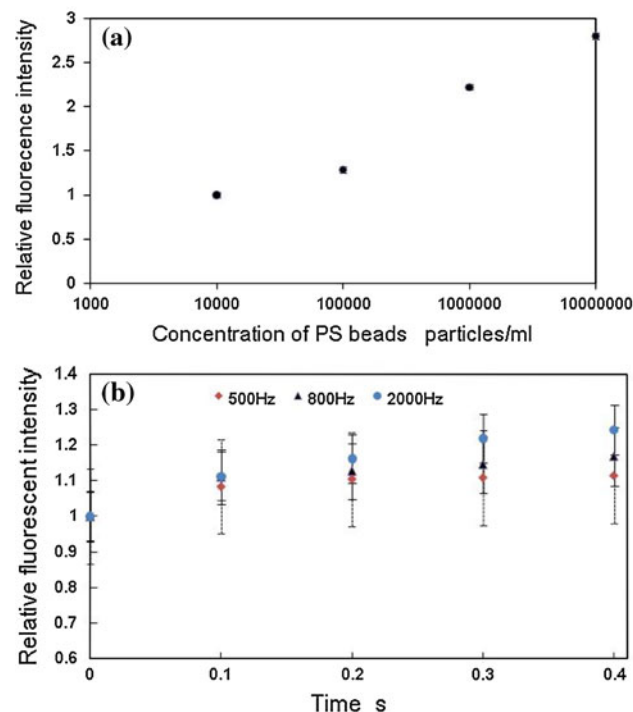


Fig. 7 Relationship between PS bead concentration and DEP frequency (based on 10^4 particles/ml). **a** Calibration results. **b** Concentration of PS beads depends on the frequency of applied voltage

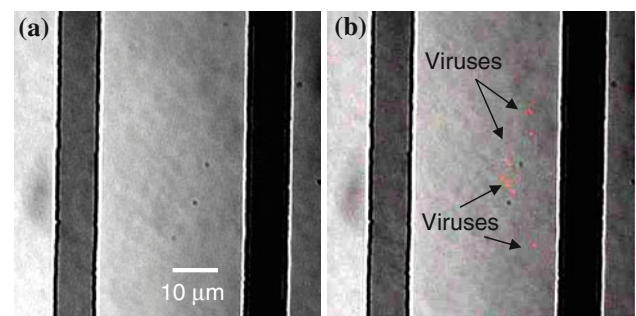


Fig. 8 Concentration of influenza viruses by DEP force. **a** Before and **b** after concentration ($20 V_{p-p}$, 3 MHz, square wave, 5 min)

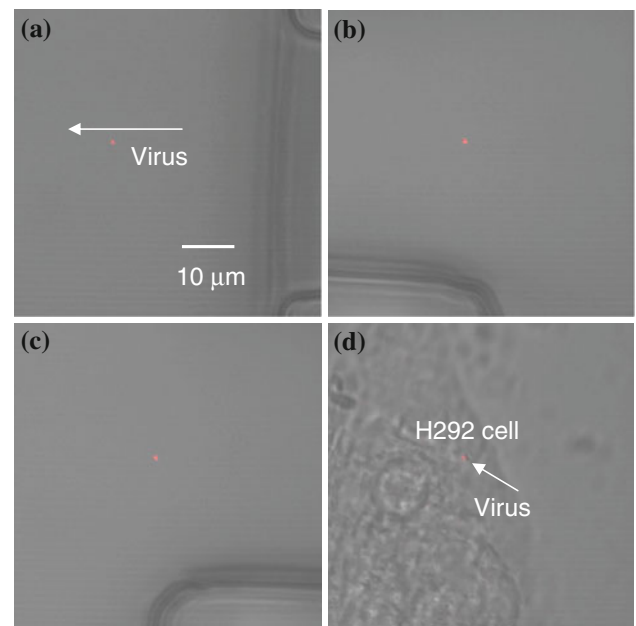
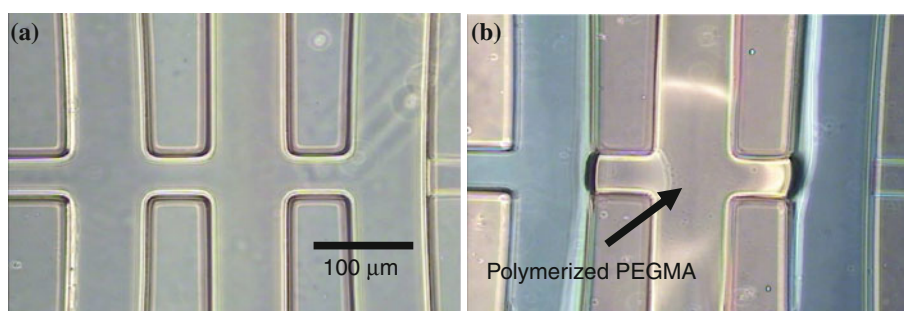


Fig. 9 Manipulation of single influenza virus and contact with an H292 cell using optical tweezers. **a** Manipulation of single influenza virus by optical tweezers ($10 \mu\text{m/s}$). **b** Transport in microchannel. **c** Transport to analysis chamber. **d** Contact with a specific H292 cell

Fig. 10 Isolation of chambers by local polymerization. **a** Before and **b** after isolation by in situ photopolymerization of photo-crosslinkable resin



We transported the virus to the analysis chamber and caused it to make contact with a selected H292 cell to infect it.

From this result, we estimated the force for transporting the virus by optical tweezers using Stokes' law:

$$F_v = 6\pi\mu r_v V_v \quad (5)$$

where F_v is driving force of the virus, μ ($= 1.002 \text{ mPa s}$) is the viscosity at 20°C , r_v is the radius of the virus, and V_v is the speed of the virus. The size of influenza viruses is considered to be in the range $80\text{--}120 \text{ nm}$ (Stanley 1944); based on this, we estimated the size of the virus to be about 100 nm . For these conditions, F_v was calculated to be 9.4 fN . The angle between the virus transport direction and the flow direction in the microfluidic chip was 90° . The trapping force of the optical tweezers is isotropic. Thus, the flow rate must be kept below $10 \mu\text{m/s}$ to be able to manipulate the virus when the laser power is 0.5 W .

Finally, the analysis chamber was isolated from the virus chamber by local photopolymerization of PEGMA to prevent other viruses from entering the cell chamber (see Fig. 10). These results demonstrate the effectiveness of our proposed system for biomedical analysis.

4 Conclusions

We have developed a system for on-chip single virus manipulation in conjunction with DEP concentration that can be used to infect a specific cell with a single virus. We concentrated viruses from 10^6 to 10^9 viruses/ μl . The negative DEP force also prevents viruses from adhering to the glass walls as well as being effective for on-chip virus manipulation. In the future, we intend to increase the throughput of biomaterial manipulation by automating the sample concentration. The concentrated viruses were manipulated by optical tweezers.

We succeeded in infecting a specific H292 cell with a single virus. The transport speed of the virus was about $10 \mu\text{m/s}$ by direct laser manipulation. This indicates that automation of single virus infection of a specific cell is possible by system integration on the microfluidic chip. Single virus infection is an essential technique for quantitative analysis of the functions of influenza viruses before

and after infection of a cell. This on-chip single virus manipulation technique has the potential to make a great contribution to biomedical applications.

Acknowledgment This work was partially supported by Core Research for Evolutional Science and Technology (CREST) of Japan Science and Technology Corporation (JST).

References

- Amato I (2005) Nanotechnologists seek biological niches. *Cell* 123:967–970. doi:10.1016/j.cell.2005.12.001
- Arai F, Ichikawa A, Ogawa M, Fukuda T, Horio K, Itoigawa K (2001) High-speed separation system of randomly suspended single living cells by laser trap and dielectrophoresis. *Electrophoresis* 22: 283–288. doi:10.1002/1522-2683(200101)22:2<283:AID-ELPS283>3.0.CO;2-C
- Arai F, Ichikawa A, Fukuda T, Katsuragi T (2003) Isolation and extraction of target microbes using thermal sol–gel transformation. *Analyst* 128:547–551. doi:10.1039/b212919a
- Arai F, Kotani K, Maruyama H (2009) On-chip robotics for biomedical innovation: manipulation of single virus on a chip. *Proc IEEE NANO 2009*:571–574
- Arthur A, Dziejcz JM, Bjorkholm JE, Chu S (1986) Observation of a single beam gradient force optical trap for dielectric particles. *Opt Lett* 11:288–290. doi:10.1364/OL.11.000288
- Castillo J, Dimaki M, Svendsen EW (2009) Manipulation of biological samples using micro and nano techniques. *Integr Biol* 1:30–42. doi:10.1039/b814549k
- Ichikawa A, Arai F, Yoshikawa K, Uchida T, Fukuda T (2005) In situ formation of a gel microbead for indirect laser micromanipulation of microorganisms. *Appl Phys Lett* 87:191108-1–191108-3. doi:10.1063/1.2126800
- Ichikawa A, Honda A, Ejima M, Tanikawa T, Arai F, Fukuda T (2007) In situ formation of a gel microbead for laser micromanipulation of microorganisms, DNA, and viruses. *J Robot Mechatron* 19:569–576
- Ishikawa M, Misawa H, Kitamura N, Masuhara H (1993) Poly (N-isopropylacrylamide) microparticle formation in water by infrared laser-induced photo-thermal phase transition. *Chem Lett* 22:481–484. doi:10.1246/cl.1993.481
- Kim MS, Lee HS, Suh KY (2008) Cell research with physically modified microfluidic channels: a review. *Lab Chip* 8:1015–1023. doi:10.1039/b800835c
- Kuhara M, Takeyama H, Tanaka T, Matsunaga T (2004) Magnetic cell separation using antibody binding with protein A expressed on bacterial magnetic particles. *Anal Chem* 76:6207–6213. doi:10.1021/ac0493727
- Maruyama H, Arai F, Fukuda T, Katsuragi T (2005) Immobilization of individual cells by local photo-polymerization on a chip. *Analyst* 130:304–310. doi:10.1039/b415400m

- Maruyama H, Arai F, Fukuda T (2008) On-chip pH measurement using functionalized gel-microbeads positioned by optical tweezers. *Lab Chip* 8:346–351. doi:[10.1039/b712566f](https://doi.org/10.1039/b712566f)
- Müller T, Fiedler S, Schnelle T, Ludwig K, Jung H, Fuhr G (1996) High frequency electric fields for trapping of viruses. *Biotechnol Tech* 10:221–226. doi:[10.1007/BF00184018](https://doi.org/10.1007/BF00184018)
- Parvin DJ, Palese P, Honda A, Ishihama A, Krystal M (1989) Promoter analysis of influenza virus RNA polymerase. *J Virol* 63:5142–5152
- Schnelle T, Müller T, Gradl G, Shirly GS, Fuhr G (2000) Dielectrophoretic manipulation of suspended submicron particles. *Electrophoresis* 21:66–73. doi:[10.1002/\(SICI\)1522-2683\(20000101\)21:1<66:AID-ELPS66>3.0.CO;2-A](https://doi.org/10.1002/(SICI)1522-2683(20000101)21:1<66:AID-ELPS66>3.0.CO;2-A)
- Shinya S, Yamanishi Y, Arai F (2009) Magnetically driven microtools actuated by a focused magnetic field for separating of microparticles. *J Robot Mechatron* 21:209–215
- Stanley MW (1944) The size of influenza virus. *J Exp Med* 79:267–283. doi:[10.1084/jem.79.3.267](https://doi.org/10.1084/jem.79.3.267)
- Yamanishi Y, Sakuma S, Onda K, Arai F (2008) Biocompatible polymeric magnetically driven microtool for particle sorting. *J Micro Nano Mechatron* 4:49–57. doi:[10.1007/s12213-008-0009-7](https://doi.org/10.1007/s12213-008-0009-7)